

An Integrated Sensor for Pressure, Temperature, and Relative Humidity Based on MEMS Technology

Jonghwa Won

*Samsung Advanced Institute of Technology, Display lab.,
P.O. Box 111, Suwon, Korea*

Sung-Hoon Choa*

*Samsung Advanced Institute of Technology, Nano-Device lab., Korea,
P.O. Box 111, Suwon, Korea*

Zhao Yulong

*Institute of Precision Engineering, Xi'an Jiao tong University,
Xi'an 710049, China*

This paper presents an integrated multifunctional sensor based on MEMS technology, which can be used or embedded in mobile devices for environmental monitoring. An absolute pressure sensor, a temperature sensor and a humidity sensor are integrated in one silicon chip of which the size is 5 mm×5 mm. The pressure sensor uses a bulk-micromachined diaphragm structure with the piezoresistors. For temperature sensing, a silicon temperature sensor based on the spreading-resistance principle is designed and fabricated. The humidity sensor is a capacitive humidity sensor which has the polyimide film and interdigitated capacitance electrodes. The different piezoresistive orientation is used for the pressure and temperature sensor to avoid the interference between sensors. Each sensor shows good sensor characteristics except for the humidity sensor. However, the linearity and hysteresis of the humidity sensor can be improved by selecting the proper polymer materials and structures.

Key Words : Integrated Sensor, Multifunctional Sensor, MEMS, Pressure, Temperature, Humidity

1. Introduction

Recently, there is an increasing demand to make sensors smaller and smaller. MEMS-based integrated sensor has the advantages of low weight, small size, low cost, and easy integration and production. Researchers are trying to integrate the whole sensor system on a single chip. Thus it will be possible to measure and evaluate all interesting

parameters for a certain task at one place and at one time. Pressure, temperature and relative humidity are the basic parameters to be required in environmental and health monitoring systems (Fujita et al., 2002; Fang et al., 2004). In these days, there is a demand that people try to understand and monitor their health status and environmental conditions by using the mobile devices such as a mobile phone and PDA. Therefore, it is very meaningful to develop the smart integrated sensors that have small volume, light weight, low power consumption. The integration of three sensors into a single substrate, so called a multifunctional sensor, is a vital challenge since it requires the integration of fabrication process, and more importantly adequate sensor performance should be maintained.

* Corresponding Author,

E-mail : shchoa@samsung.com

TEL : +82-31-280-9455; FAX : +82-31-280-9473

Samsung Advanced Institute of Technology, Nano-Device lab., Korea, P.O. Box 111, Suwon, Korea. (Manuscript Received October 10, 2005; Revised February 7, 2006)

In this study, we have designed and fabricated a new MEMS-based integrated sensor which can be used or embedded in the mobile devices, such as the mobile phone, to monitor the environmental conditions. Absolute pressure, temperature, and relative humidity sensor have been monolithically integrated as a single chip. In particular, we focus on making the integrated sensor as small as possible due to the size limitation in the mobile phone application. In this study, the absolute pressure sensor is based on piezoresistance technology (Guckel, 1991; Zhao et al., 2003; Lee et al., 2006). The temperature sensor adopts a spreading-resistance method (Obermeier et al., 1992; Lai et al., 1999), and the humidity sensor employed an interdigitated capacitive sensing method (Story et al., 1995; Matsuguch et al., 1998).

2. Sensor Design and Theory of Operation

2.1 Pressure sensor

Figure 1 show the structure of the absolute pressure sensor which is designed to measure the atmospheric pressure. The absolute pressure sensor uses a bulk-micromachined diaphragm structure, and it forms the vacuum chamber with the glass substrate, which is commonly known as a piezoresistive pressure sensor (Shim et al., 2004). The silicon structure wafer and Pyrex glass wafer are bonded by an anodic bonding method in a vacuum condition. The piezoresistors placed on the diaphragm form a full bridge and provide the voltage output according to the induced strain from the ambient pressure. The membrane is fabricated by etching away the bulk silicon in a defined region until a required thickness is reached. Piezoresistance is made by boron implantation into the n-type silicon membrane, which results in the p-type polysilicon. In this study, the conditions of the boron ion implantation are the dose of $2.0 \times 10^{15} \text{ cm}^{-2}$ and energy of 80 keV. Because of the implanted boron ion and the n-type bulk silicon, a pn-junction is formed between the boron ion field and n-type silicon. The value of piezoresistance is about 25Ω per square of the piezoresistance width ($25\Omega/\square$) in order

to get higher piezoresistors as the pressure is applied to the sensor. All the four piezoresistances of the pressure sensor are formed the Wheatstone bridge circuit. The pressure signal can be obtained through the strain of the piezoresistors. In order to achieve the maximum sensitivity of the pressure sensor, the dimension of diaphragm should be carefully determined and optimized. From the stress analysis by the finite element method using ANSYS software, it can be seen that the maximum stress occurs at the center area of each membrane edge as shown in Fig. 2. Therefore, piezoresistors are located at those areas. In addition, the size of the membrane is optimized using finite element method. The final size of the pressure sensor is $1.5 \text{ mm} \times 1.5 \text{ mm}$ with the diaphragm thickness of $25 \mu\text{m}$.

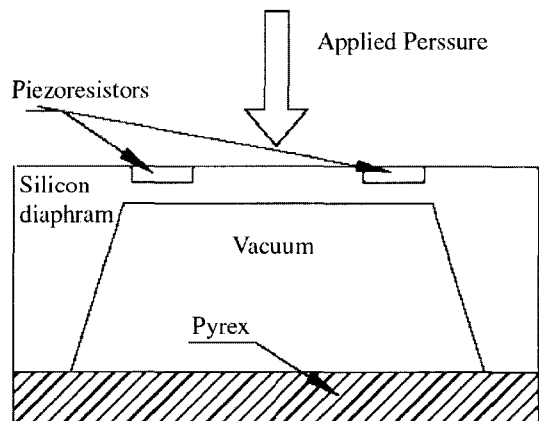


Fig. 1 Structure of the absolute pressure sensor

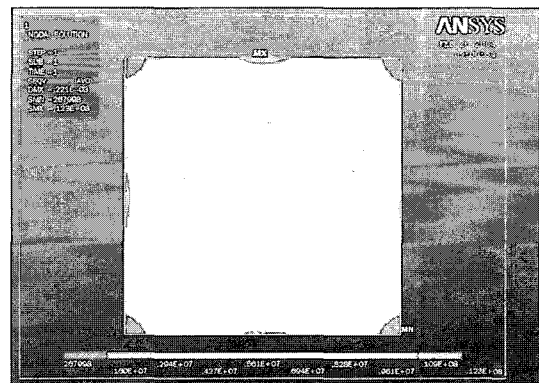


Fig. 2 Stress distribution of the diaphragm by the finite element method

2.2 Temperature sensor

The temperature sensor used in this study is the spreading-resistance temperature (SRT) sensor which has been proposed for over ten years (Obermeier et al., 1992). Silicon temperature sensors based on this spreading resistance principle can work at temperature from -65°C to 300°C . The brief operation principle of SRT sensor can be described as follows :

The resistivity (ρ) of semiconductor of the temperature sensor can be expressed as follow :

$$\rho = \frac{1}{nq\mu_n + pq\mu_p} \quad (1)$$

Where, μ_n and μ_p are the mobility of the n-type and p-type carriers, respectively. And p is the concentration of boron ion and q is the charge of free electron, respectively. When the boron ion implantation (or p-type silicon) is performed, the Eq. (1) can be expressed as :

$$\rho = \frac{1}{pq\mu_p} \quad (2)$$

since $n\mu_n \ll pq\mu_p$.

As above, it can be seen that the concentration and the mobility of carriers (electron or hole) determine the resistivity of semiconductor. It is also to say that the resistivity depends on impurity concentration of the carrier. This is the base of the implantation of boron ion to the n-type silicon wafer. Furthermore the resistivity of the silicon is related to temperature, and it can be shown as Eq. (3):

$$\rho(T) \approx \frac{1}{T} \exp \left[\frac{E_g(0) - \frac{(4.73 \times 10^{-4}) T^2}{T + 636}}{2kT} \right] \quad (3)$$

where, T is the measured temperature in Kelvin, k is the boltzmann constant ($1.38 \times 10^{-23}\text{J/K}$) and E_g is the band edge of silicon at $T=0\text{ K}$ (1.17eV). Therefore the resistivity of semiconductor will be changed as the temperature varies for certain impurity concentration according to Eqs. (2) and (3). In this study, conditions of the boron ion implantation are the same as those used in the pressure sensor since the boron ion implantation is conducted simultaneously for both of the pressure sensor and the temperature

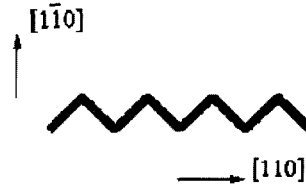


Fig. 3 Structure of the temperature sensor

sensor. The structure of the temperature sensor is illustrated in Fig. 3. It has a zigzag pattern to increase the sensitivity of the sensor and to avoid interference with the pressure sensor. The detail reason for this zigzag pattern for the temperature sensor will be discussed in the next section. The width and the length of the temperature sensor's resistance are $8\ \mu\text{m}$ and $2400\ \mu\text{m}$, respectively.

2.3 Humidity sensor

The humidity sensor used in this study is a capacitive humidity sensor which is commonly used because of its relatively good linear sensitivity in a wide range of relative humidity (Story et al., 1995). The sensing principle of the humidity sensor is based on the dielectric constant change of the deposited polyimide due to absorption of water vapor. The sensing element is based on the interdigitated (IDT) capacitance electrodes. The electrodes are made from the aluminum layers. And the polyimide film is coated on the interdigitated capacitance electrodes. The capacitance (C) of the humidity sensor will be changed as the dielectric constant of the polyimide film is changed because of the absorption of water vapor. And the absorption of water vapor is mainly due to the environment humidity. The capacitance of the humidity sensor can be illustrated as :

$$C = \frac{\epsilon_0 \epsilon_r S}{d} \quad (4)$$

where

d is the distance between interdigitated electrodes.

S is the plate area of the capacitor, which determined by size of the interdigitated electrodes.

ϵ_0 is the permittivity of vacuum ($8.85\ \text{pF/m}$).

ϵ_r is relative permittivity of polyimide sensing material.

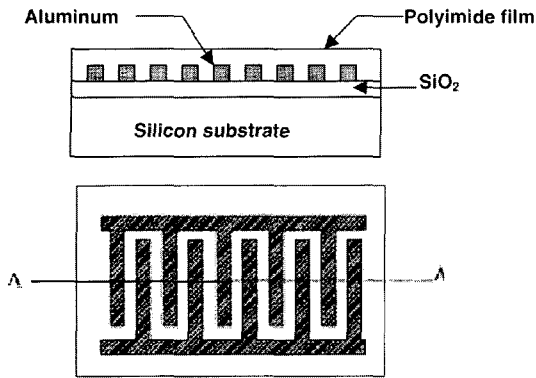


Fig. 4 Structure of the humidity sensor

The dielectric constant of the polyimide film and water are equal to 2.93 and 80, respectively. The absorbed water causes changes in permittivity and impedance of the polyimide film, which can be detected by capacitance changes. The more water the polyimide film absorbs, the larger the value of ϵ_r becomes. The structure of the humidity sensor is shown in Fig. 4. There are 49 pairs of Al electrodes in the humidity sensor. The effective length and width of the Al electrodes are $500 \mu\text{m}$ and $8 \mu\text{m}$, respectively. The separation distance of two electrodes is $2 \mu\text{m}$. A layer of $1.2 \mu\text{m}$ thick aluminum is sputtered on the substrate and then patterned.

3. Device Design and Fabrication

It is well known that there is anisotropy characteristics along different orientation of the single crystal silicon. In this study, an integrated sensor chip is processed from an n-type 4 inch silicon wafer with (100) orientation. The piezoresistors in the pressure sensor and the temperature resistance are realized through p-type polysilicon doped by the boron ion implantation. There is the largest piezoresistance coefficient along the crystal direction $[110]$ or $[\bar{1}\bar{1}0]$. To maximize the sensitivity of the sensor, the piezoresistive sensor is located in $[\bar{1}\bar{1}0]$ orientation. On the other hand, there is almost no piezoresistance coefficient along the crystal direction $[100]$ and $[010]$ in (100) silicon. Therefore, the temperature resistor is located along the direction $[100]$ and

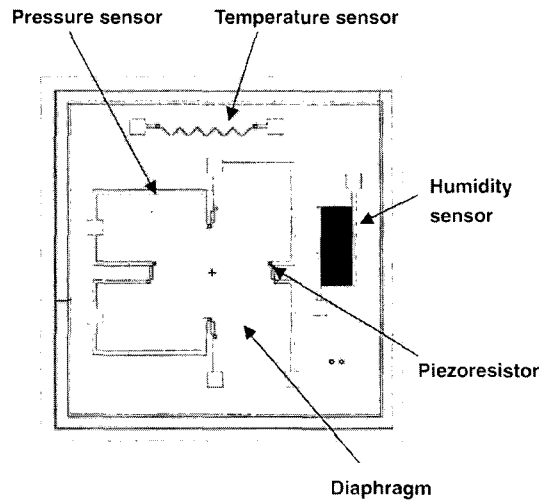


Fig. 5 Schematic diagram of an integrated sensor chip

$[010]$ in order to avoid the interference between the pressure sensor and temperature sensor. Therefore the temperature sensor has the zigzag pattern as shown in Fig. 3. It is to say, the $[110]$ direction is used for the piezoresistor of pressure sensor, while the $[100]$ direction is employed for the temperature sensor. For the humidity sensor, there is the least interference with the pressure sensor and the temperature sensor, and vice versa. The integrated structure of the sensor chip is shown as Fig. 5. The total size of the integrated sensor chip is $5 \text{ mm} \times 5 \text{ mm}$.

The fabrication process of the integrated sensor is shown in Fig. 6. The fabrication is started with the deposition of 800 nm thick thermal oxide on the silicon wafer. After patterning of the thermal oxide, the boron ion is implanted to the substrate. This forms resistors patterns of the pressure sensor and temperature sensor, which has the resistance of around $25 \Omega/\square$. A Si_3N_4 layer with depth of 120 nm is formed using Low Pressure Chemical Vapor Deposition (LPCVD) to protect the circuit of the sensors. Then the backside of the substrate is etched away to form a $25 \mu\text{m}$ thick diaphragm. An aluminum film of $1.2 \mu\text{m}$ thick is sputtered to form the interdigitated electrode and the metal pads for electrical connection in the chip. Then the silicon and Pyrex glass are bonded together in vacuum condition through anodic bonding process. This package

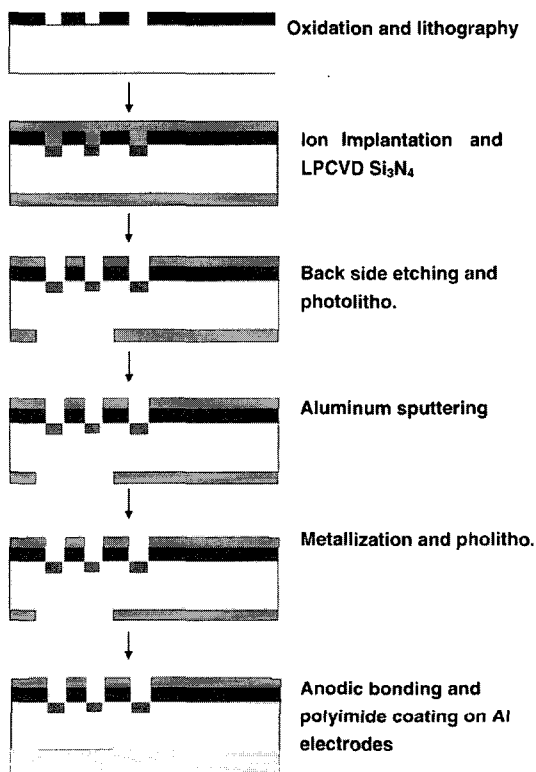


Fig. 6 Simplified fabrication process flow of the integrated sensor chip

forms the vacuum cavity of the pressure sensor for the absolute pressure measurement. Finally, the polyimide film was spun onto the interdigitated electrodes.

4. Experimental Results

In order to investigate the characteristics of the pressure sensor, a piston pressure meter was used, which is shown in Fig. 7. The measurement range of the piston pressure meter is from 0.1 kPa to 250 kPa. However, pressure was measured from 0.1 kPa to 101 kPa since we were only interested in pressure lower than the atmospheric pressure. Figure 8 shows the output voltage versus the applied pressure. The sensitivity of the pressure sensor is approximately 2.11 mV/kPa. Constant voltage of 5 V and constant current of 1.5 mA are supplied into the sensor chip. The main characteristics of the pressure sensor are listed in Table 1. For the temperature sensor, the

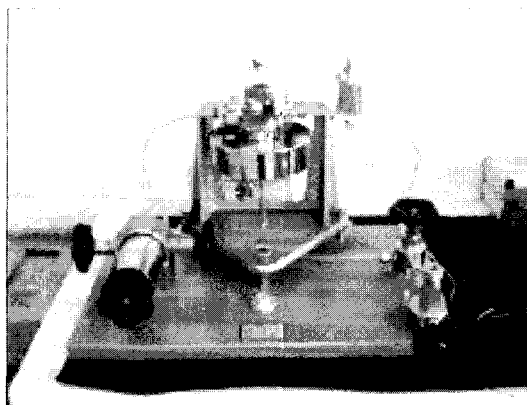


Fig. 7 Picture of the piston pressure meter for testing the pressure sensor

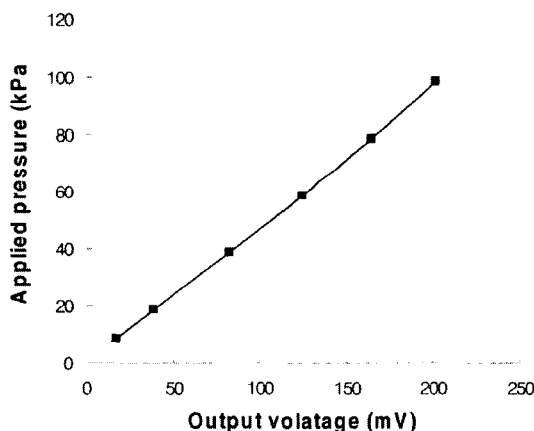


Fig. 8 Relationship between pressure and output voltage in the pressure sensor

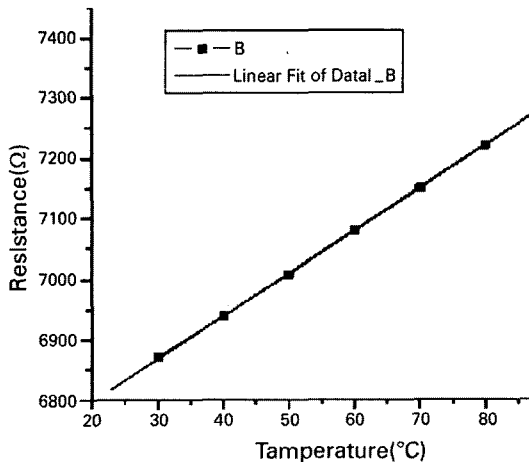
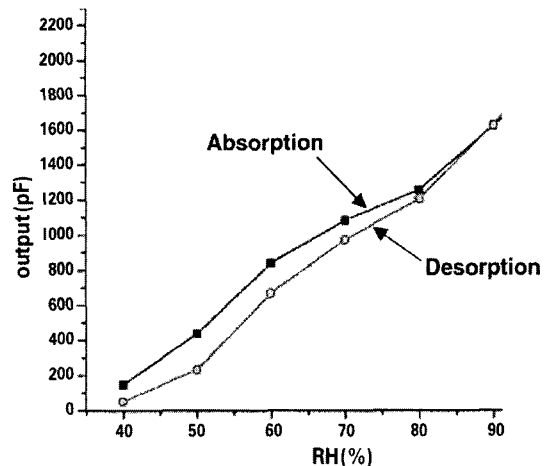
temperature controllable chamber was used to investigate the characteristics of the temperature sensor. Multimeter was used to measure the resistance of the temperature sensor. Figure 9 shows the resistance change for various temperatures. The characteristics of the temperature sensor are also listed in Table 1.

For the humidity sensor test, saturated salt solutions were used to generate an environment of a particular relative humidity in an enclosed space. Since the value of relative humidity obtained depends on the particular chemical salt such as magnesium chloride, magnesium nitrate, sodium chloride, and the concentration of the salt solution, we can control the relative humidity by

Table 1 Characteristics of each sensor in an integrated chip

	Pressure Sensor	Temperature	Humidity Sensor
Linearity	$\pm 0.165\%FS$	$\pm 0.6\%FS$	5.3%FS
Sensitivity	2.11 mV/kPa	11.3 $\Omega/^\circ C$	30 pF/%RH
Hysteresis	$\pm 0.186\%FS$	$\pm 0.8\%FS$	10.2%FS
Tested Range	0.1 kPa~101 kPa	0 $^\circ C$ ~90 $^\circ C$	32~100%RH

(FS : full scale)

**Fig. 9** Relationship between temperature and resistance in the temperature sensor**Fig. 10** Relationship between relative humidity and output capacitance in the humidity sensor

using different saturated salts and different concentrations. The saturated salt solution is placed in the glass container with a commercially available humidity sensor. Then the integrated sensor chip was located inside the glass container, and glass container was sealed. It takes some time (2 to 6 hours) for the air inside the container to reach the proper relative humidity level. After the first calibration curve was obtained, above procedures were repeated in order to determine the second calibration point using different saturated salt solutions. The relative humidity data for each saturated solution and concentration can be easily obtained from the table in Ref. (Center for microcomputer applications, 2003). Figure 10 shows the relationship between the capacitance changes with relative humidity during absorption and desorption. Digital capacitance meter is used to monitor the capacitance change of the humidity sensor. The linearity of the humidity sensor is 5.3%FS (full scale) and hysteresis is 10.2%FS.

The values of linearity and hysteresis of the humidity sensor in this study are not good as much as those presented in other researches (DeHennis et al., 2005 ; Laconte et al., 2003) . However it was known that the performances of the humidity sensor could be improved by selecting the proper polymer material and structures (Dokmeci et al., 2001 ; Laconte et al., 2003) . Therefore we think that we can further improve the performances of the humidity sensor.

In this study, the interferences between each sensor were not studied in details. For example, it is thought that the sensitivity of the piezoresistive sensor would be influenced by temperature, and the temperature sensor would be influenced by relative humidity, and vice versa. However, the main objective of this study is to find feasibility of the integrated single chip sensor of which the main target application is the mobile devices which require the small size, low cost, and low power consumption rather than higher sensitivity.

Therefore the detailed study of the interference between sensors will be conducted as one of the future work. Also we used the resistance detection method for pressure and temperature sensing, on the while the capacitance detection method for humidity sensing. In order to simplify the sensing circuit, resistance detection method as for the humidity sensor will be studied in the future.

5. Conclusions

This paper has reported the design, fabrication and characterization of an integrated multifunctional sensor for measuring absolute pressure, temperature, and relative humidity. We focused on the development of an integrated sensor chip which has the small size and low cost for application in the mobile devices for environmental monitoring. The sensors were fabricated with monolithic process based on MEMS technology. The each sensor shows relatively good sensor characteristics including linearity, sensitivity and hysteresis except for the humidity sensor. The pressure sensor has the linearity of 0.165%FS and sensitivity of 2.11 mV/kPa. The linearity and sensitivity of the temperature sensor are 0.6%FS and 11.3 Ω /°C, respectively. The humidity sensor shows the linearity of 5.3%FS, sensitivity of 30 pF/%RH, and hysteresis of 10.2%FS, respectively. The linearity and hysteresis of the humidity sensor are not satisfactory at this point. However, it can be improved by selecting the proper polymer materials and structures. The final size of the integrated sensor chip was 5 mm \times 5 mm.

References

- Center for Microcomputer Applications, Universiteit van Amsterdam, 2003, "Relative Humidity Sensor," (<http://www.cma.science.uva.nl/english/download/pdf/manuals/d025i.pdf>).
- DeHennis, A. D. and Wise, K. D., 2005, "A Wireless Microsystem for the Remoting Sensing of Pressure, Temperature, and Relative Humidity," *Journal of Microelectromechanical Systems*, Vol. 14, No. 1, pp. 12~22.
- Dokmeci, M. and Najafi, K., 2001, "A High-Sensitivity Polyimide Capacitive Relative Humidity Sensor for Monitoring Anodically Bonded Hermetic Micropackages," *Journal of Microelectromechanical Systems*, Vol. 10, No. 2, pp. 197~204.
- Fang, Z., Zhao, Z., Wu, Y., Zhang, B. and Wang, Y., 2004, "Integrated Temperature and Humidity Sensor Based on MEMS," *Proc. of International Conference on Information Acquisition*, pp. 84~87.
- Fujita, T. and Maenaka, K., 2002, "Integrated Multi-Environmental Sensing-System for the Intelligent Data Carrier," *Sensors and Actuators A*, Vol. 97-98, pp. 527~534.
- Guckel, H., 1991, "Surface Micromachined Pressure Transducers," *Sensors and Actuators A*, Vol. 28, No. 2, pp. 133~146.
- Laconte, J., Wilmart, V., Flandre, D. and Raskin, J.-P., 2003, "High-Sensitivity Capacitive Humidity Sensor Using 3-Layer Patterned Polyimide Sensing Film," *Proc. of IEEE Sensors*, Vol. 1, pp. 22~24.
- Lai, P. T., Bin Li, C. L. and Sin, J. K. O., 1999, "Spreading-Resistance Temperature Sensor on Silicon-On-Insulator," *IEEE Electron Device Letters*, Vol. 20, No. 11, pp. 589~591.
- Lee, S., Kim, J. and Shin, Y., 2006, "The Influence of Residual Stress on the Frequency of Ultrasonic Transducers with Composite Membrane Structure," *Journal of Mechanical Science and Technology*, Vol. 20, No. 1, pp. 76~84. (in Korea)
- Matsuguch, M., Kuroiwa, T., Miyagishi, T., Suzuki, S., Ogura, T. and Sakai, Y., 1998, "Stability and Reliability of Capacitive-Type Relative Humidity Sensors Using Crosslinked Polyimide Films," *Sensors and Actuators B*, Vol. 52, pp. 53~57.
- Obermeier, E. and Kopystinsky, P., 1992, "Polysilicon as a Material for Microelectronic Applications," *Sensors and Actuators A*, Vol. 30, pp. 149~155.
- Shim, J. J., Han, G. J. and Han, D. S., 2004, "Evaluation of the Residual Stress with Respect to Supporting Type of Multi-layer Thin Film for the Metallization of Pressure Sensor," *Transactions of the Korean Society of Mechanical Engi-*

neers A, Vol. 28, No. 5, pp. 532~538. (in Korea)
Story, P. R., Galipeau, D. W. and Mileham, R. D., 1995, "A Study of Low-Cost Sensors for Measuring Low Relative Humidity," *Sensor and Actuators B*, Vol. 24-25, pp. 681~685.

Zhao, Y. L., Zhao, L. B. and Jiang, Z. D., 2003, "A Novel High Temperature Pressure Sensor on the Basis of SOI layers," *Sensors and Actuators A*, Vol. 108, pp. 108~111.